Geomatica 76 (2024) 100037

Contents lists available at ScienceDirect

Geomatica

journal homepage: www.sciencedirect.com/journal/geomatica

Spatial scale drives pedodiversity-elevation relationship in Botswana☆

Ndiye Michael Kebonye[a,b,*], Ruhollah Taghizadeh-Mehrjardi[a,c], Kingsley John[d], Prince Chapman Agyeman[e], Nafiseh Kakhani[a,c], Zibanani Seletlo[f], Lesego Motlhetlhi[g], Boineelo Moyo[h], Thomas Scholten[a,b,c]

[a] Department of Geosciences, Chair of Soil Science and Geomorphology, University of Tübingen, Rümelinstr. 19–23, Tübingen, Germany
[b] DFG Cluster of Excellence "Machine Learning: New Perspectives for Science", University of Tübingen, AI Research Building, Maria-von-Linden-Str. 6, 72076 Tübingen, Germany
[c] CRC 1070 Resource Cultures, University of Tübingen, Tübingen, Germany
[d] Department of Plant, Food, and Environmental Sciences, Faculty of Agriculture, Dalhousie University, Cox Institute Building, 50 Pictou Rd., PO Box 550, Truro, NS, B2N 5E3, Canada
[e] Sustainable Resource Management, Memorial University of Newfoundland, Corner Brook A2H 6P9, Canada
[f] Department of Animal Science and Production, Faculty of Animal and Veterinary Sciences, Botswana University of Agriculture and Natural Resources, Private Bag 0027, Gaborone, Botswana
[g] Department of Earth and Environmental Science, Faculty of Science, Botswana International University of Science and Technology, Private Bag 16, Palapye, Botswana
[h] Thünen Institute of Rural Studies, Bundesallee. 50, 38116 Braunschweig, Germany

ARTICLE INFO

Keywords:
Landscape ecology
Pedodiversity
Botswana
RaO's quadratic entropy
Soil-forming factors
Spatial scale

ABSTRACT

Elevational distribution affects pedodiversity (a measure or indicator of soil diversity) by controlling factors like climate, vegetation, and water drainage. It plays a vital role as a constant variable in soil formation processes (*e.g.*, mineralization, eluviation, and illuviation, *etc.*) thus promoting diverse soil types at different toposequence formations. However, the relationship between pedodiversity and elevation at various spatial scales remains poorly understood and obscure, especially for dryland regions. Here, we first derive a national-scale pedodiversity map of Botswana, explaining more than 50 % of the variance. For this map, elevation is among the most important environmental covariates influencing soil diversity. We further examine how spatial scale indicators such as spatial extent (*i.e.*, countrywide, and locally) and resolution (*i.e.*, 90 m, 900 m, 9000 m, and 90,000 m) systematically influence landscape pedodiversity. While viewing the data countrywide, the relationship between pedodiversity and elevation maintained a negative or inverse linear trend (*i.e.*, meaning that as elevation increases, pedodiversity decreases), but when viewed locally—for the small district, it showed a positive or direct linear trend (*i.e.*, both elevation and pedodiversity increase simultaneously). This can be explained by differences in elevation patterns together with complex and dynamic interactions between scale-dependent soil-forming factors like land use type which tend to dominate local scales. Significant differences in pedodiversity related to the spatial resolution of geodata inputs were noticeable, for example, the local coefficient of determination values ranged from 0.06 to 0.65 for fine to coarse spatial resolutions respectively. Together, our findings demonstrate that the relationships between pedogenesis factors (*e.g.* elevation) and pedodiversity are scale-dependent. Even a small change in spatial resolution can lead to significant variations in pedodiversity, especially in semi-arid areas. Therefore, taking this into account can reduce overly optimistic conclusions about the landscape patterns we observe.

1. Introduction

Landscape patterns and relationships between landscape features (*e.g.*, soils, rock or geological outcrops, waterbodies, vegetation, *etc.*) and their forming factors largely determine the diversity of a landscape and are crucial to understanding soil-landscape evolution. Further, ecological processes (*e.g.*, nutrient cycling, and soil respiration) are interconnected with landscape patterns and diversity in various ways. For

☆ The first and last authors hold designated positions; the order of authors in between does not follow a specific sequence.

* Corresponding author at: Department of Geosciences, Chair of Soil Science and Geomorphology, University of Tübingen, Rümelinstr. 19–23, Tübingen, Germany.
E-mail address: ndiye.kebonye@uni-tuebingen.de (N.M. Kebonye).

https://doi.org/10.1016/j.geomat.2024.100037
Received 13 October 2024; Received in revised form 8 November 2024; Accepted 21 November 2024
Available online 22 November 2024

example, nutrient cycling involves the movement and exchange of nutrients such as carbon, nitrogen, and phosphorus within an ecosystem, which can influence plant diversity and contribute to the formation of unique soils. Previous studies by [1,2] have examined the connections between geodiversity (which includes soils) and biodiversity, as well as ecosystem productivity and biodiversity, to better understand overall ecosystem functioning. These studies have shown that ecological connections strongly depend on the spatial scale, meaning that even small changes in spatial resolution, extent, or combination can lead to unique landscape patterns and relationships.

Although soil diversity, which we will later refer to as pedodiversity, is part of geodiversity, the two concepts focus on different components. Geodiversity encompasses a broader range of natural diversity, including geology, topography, and soils, combined into a single indicator for decision-making [3,4]. Meanwhile, pedodiversity specifically describes the diversity of soil classes or taxonomic units in a specific geographical area [5]. Pedodiversity has been theorized over time and almost studied extensively in general [6–9], for different types of landscapes, for example, high mountain ranges in China [10] and on a country base for the USA [11], Germany [12], and Czechia [13]. Additionally, other studies explore the role of pedodiversity in biodiversity [14].

Major factors driving or controlling pedodiversity are geomorphological characteristics or units plus other environmental factors like climate, biota, parent material, and age [15]. Human activities also have an essential influence on the formation of various soils; for example, the formation of Technosols is primarily associated with the human footprint [16]. Pedodiversity can be analyzed mathematically through known indices such as Shannon's entropy index and RaO's quadratic entropy index or directly assessed using soil parameters like texture, pH, and microbial communities or populations [13,17,18]. Most studies analyze pedodiversity based on soil classes since these explain the overall variability associated with soil-forming factors and chemical, biological, and physical soil parameters. For instance, Arenosols found in dryland environments typically have high sand content, low exchangeable bases, low nutrient levels, and relatively low microbial activity [19,20]. These soils dominate most land masses, particularly in areas like Namibia, Botswana, Australia, and Iran [21]. In some of these dry places, pedodiversity is often quantified as low presumably due to the arid climatic conditions and delayed or slow pedogenetic processes when compared to mesic regions [22,23]. We also observe low pedodiversity estimates based on the Shannon entropy in dryland regions at the global scale [24].

Despite the low pedodiversity and low diversity of soil organisms in dryland regions, it is important to study their relationship with other aspects of the landscape, such as ecosystem services, biodiversity, and elevation changes. This is crucial for environmental and natural resource conservation efforts, as well as for monitoring trends and related changes in the physical structures of the area. It becomes apparent that understanding pedodiversity patterns is important for various landscape decisions such as the need to delineate suitable agricultural land for production [9], which is especially important in dry environments.

However, while making landscape decisions, it is important to consider various constraints when connecting pedodiversity to other landscape aspects. For example, one challenge of using pedodiversity to describe the variation of soil classes in a specific area is the wide range of physical, chemical, and biological properties expected within individual soil units, such as a single type of soil that can have a texture ranging from sandy to clayey at the same time. This is particularly important when using vector-based soil class maps with distinct boundaries in the form of multi-polygons. This constraint has been found to limit efforts to link pedodiversity to ecosystem services in France, that is, considered not straightforward [25]. Another key issue is scale dependence, which is likely to affect the relationship between pedodiversity and other landscape aspects in the same way as ecological relationships like geodiversity-biodiversity and ecosystem productivity-biodiversity [1,2]. Vašát et al. [13] investigated pedodiversity and attempted to account for scale dependency. However, their study only examined the spatial structure of pedodiversity nationally and did not relate it to any other landscape aspect. Understanding the relationship between pedodiversity and other landscape features like elevation can reveal changes in soil patterns. For example, differences in soil colour at different elevations can indicate variations in biogeochemical processes in soils [26]. This knowledge may also be relevant to other areas of research, such as ecology and biogeography [27], aiming to increase interdisciplinary understanding of overall landscape diversity-related aspects, including biodiversity, plant growth, sediment transport, *etc.*

Different factors such as climate, human activities, geographic position, vegetation, and geology influence pedodiversity. Here, we focus on elevation as a key factor that influences pedodiversity and various soil processes, such as humification and nutrient cycling. Elevation also affects climatic conditions, vegetation, and soil class variability. The connection between pedodiversity and elevation is sometimes studied, but researchers often only consider a one-sided relationship between the two factors without considering variations in spatial scale. Vacek et al. [9] found that pedodiversity decreased with an increase in elevation in forested high-altitude areas of the Czech Republic. Meanwhile, in Mexico, pedodiversity was observed to increase with elevation because of erosion occurrences at higher altitudes under semideciduous forests [28]. The two studies indicate opposing outcomes regarding the pedodiversity-elevation relationship, which remains unresolved. Aside from that, none of these studies analyzed the scale-dependent effects associated with this relationship, a research gap that has received little attention thus far despite its relevance in helping shed light on the understanding of overall landscape diversity and ecological functioning [29]. By scale dependence here we refer to aspects of spatial scale, the extent of a given area and resolution, and how varying each could potentially influence pedodiversity dependence on elevation. The term scale is well-validated and widely used in the digital soil mapping (DSM) literature and community [30–32]. These studies demonstrate scenarios where the extent and resolution are varied across different places to monitor and analyze changes in landscape interactions derived through models.

Thus, to address these fundamental research gaps, we ask the main question of whether varying the spatial extent, here from countrywide to district levels as well as resolution would affect the pedodiversity-elevation relationship in semi-arid Botswana and how. Assessing the pedodiversity-elevation relationship in such semi-arid environments is particularly important because of its implications for agriculture, environmental management, and understanding ecological processes. Our specific objectives were to (1) create a fine-resolution (90 m) soil class map of Botswana and use it to estimate pedodiversity, (2) evaluate pedodiversity-elevation relationships in Botswana at varying spatial extents and resolutions as well as (3) translate our findings on these relationships for operational purposes. First, we considered four consecutive spatial resolution (*i.e.*, 90 m, 900 m, 9000 m, and 90000 m) maps of the two variables across three spatial extents in Botswana (*i.e.*, countrywide, a large Central district, and a small Southern district). The 90 m represents the fine resolution, 900 m intermediate resolution, 9000 m coarse resolution, and 90,000 m very course resolution. Moreover, this systematic approach to varying resolution is logical, enabling scale-dependent landscape relationships to be better understood. Second, we extracted pedodiversity and elevation observational data for each spatial extent and resolution mentioned above. Finally, applying conventional statistical models, we used the data to assess pedodiversity-elevation relationships. Botswana is an ecologically heterogenous semi-arid environment due to different vegetation types (*e.g.*, sandveld, hardveld, wetlands, miomboveld), rich biodiversity (*e.g.*, wildlife), and hydrological characteristics (*e.g.*, underground water reserves) [33–35]. Hence, knowledge regarding pedodiversity-elevation relationships is crucial for inferring similarities in landscape patterns and variability, especially for variables closely linked to elevational changes, for example, vegetation cover.

2. Material and methods

2.1. Study area and data sources

Our study followed the workflow illustrated in Fig. 1. Botswana lies approximately between coordinates 17̊S and 27̊S latitude and 20̊E and 30̊E longitude. This is a massive semi-arid landmass [36–38] covering an area of approximately 582,000 km^2, with undulating savanna vegetation in either the hardveld or sandveld ecoregions [39]. Hardveld and sandveld regions are characterized by varied soils ranging from loamy highly fertile and sandy less vegetated soils respectively [39–42]. The Central and Southern districts were selected based on their area size and overall landscape features, with the former covering a considerable portion of the hardveld [43] and the latter mostly comprising the sandveld ecoregion. Legacy soil class observational data for Botswana was obtained from the Africa Soil Information Service – AfSIS (https://www.isric.org/projects/africa-soil-profiles-database-afsp) [44] and the Botswana Range Inventory and Monitoring Project – BRIMP under the Ministry of Agriculture [45]. For the BRIMP data, we applied the verified soil class centroids across the entire country. Combining these datasets constituted approximately $n = 2060$ observational points (Fig. 2A). These points would be used to generate the soil class model and fine detail map (90 m resolution) based on expertly chosen covariates that influence soil processes in Botswana (Fig. 2B). These covariates in full names, abbreviations, spatial resolution, and sources are

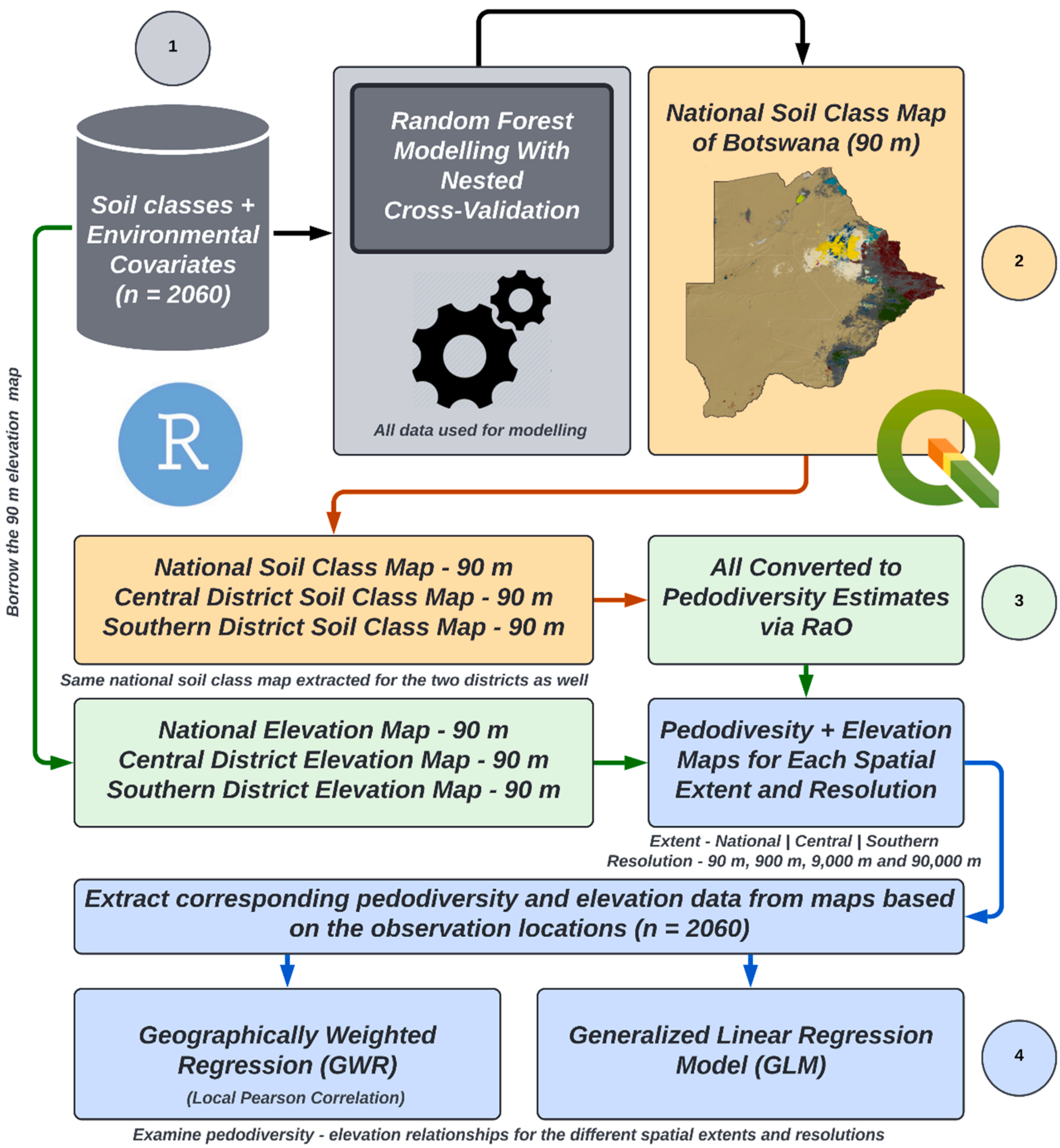

Fig. 1. Schematic showing the entire study methodology divided into several stages. [Note: Similar colours represent corresponding processes, for example, number 1 depicted in grey colour represents the first machine learning modelling phase to generate the countrywide soil class map at 90 m resolution. Phase number 2 (in orange) is the soil class maps for the three areas of interest while number 3 represents the preparation of the data matrices comprising the pedodiversity and elevation for the different spatial extents and resolutions. Number 4 in blue is the second modelling phase where the geographically weighted regression (GWR) and generalized linear regression (GLM) are applied to assess the pedodiversity-elevation interplays].

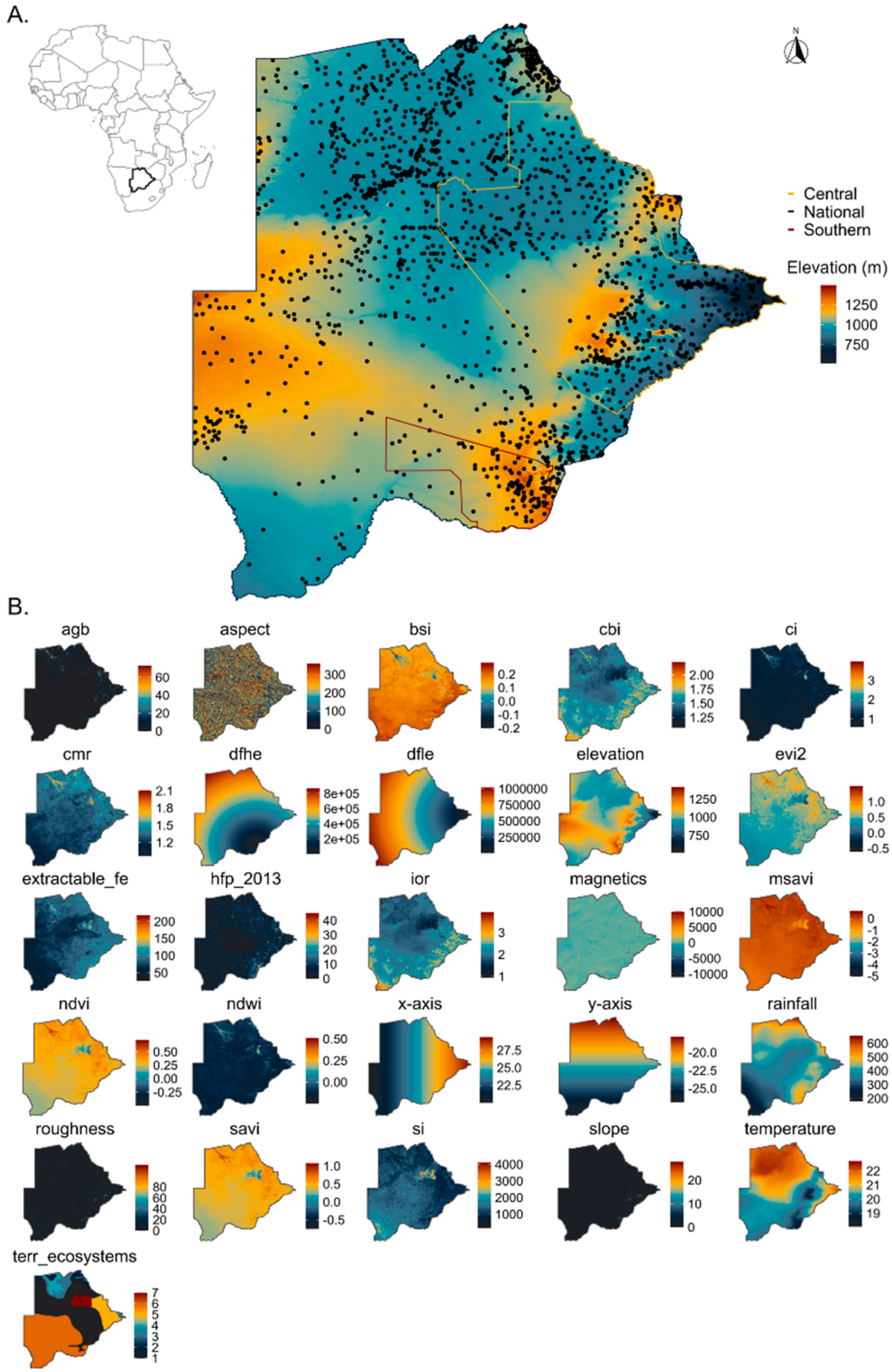

Fig. 2. Map of Botswana showing the soil class observational points (n = 2060). (a) The location of Botswana in Africa including the other study areas, Central and Southern districts all undulating on the elevation map. (b) All environmental covariates stacked together and used to model soil classes across Botswana. [Note: Full names of the covariate are: Above Ground Biomass (agb), Aspect (aspect), Bare Soil Index (bsi), Carbonate Index (cbi), Clay Index (ci), Clay Mineral Ratio (cmr), Distance from Highest Elevation (dfhe), Distance from Lowest Elevation (dfle), Elevation (elevation), Two-Band Enhanced Vegetation Index (evi2), Extractable Iron (extractable_fe), Human footprints (hfp_2013), Iron Oxide Ratio (ior), Magnetics (magnetics), Modified Soil Adjusted Vegetation Index (msavi), Normalized Difference Vegetation Index (ndvi), Normalized Difference Water Index (ndwi), Longitude (x-axis), Latitude (y-axis), Rainfall (rainfall), Roughness (roughness), Soil Adjusted Vegetation Index (savi), Salinity Index (si), Slope (slope), Temperature (temperature), Terrestrial Ecoregions (terr_ecosystems). All maps are based on the World Geodetic System (WGS) 1984 projection].

provided in Table 1.

2.2. Modelling and mapping aspects

Botswana already has an existing soil class map from the 1990s [51]. This map provides coarse scale information at 1: 1000000 (~10000 m), with vector polygons displayed as crisp boundaries separating distinct soil classes [52]. For a resolution of ~10000 m, each centimeter on the map represents 10 km in real distance. However, to relate pedodiversity and elevation across scales, we needed a fine-scale map for detailed analysis. So, rather than relying on the current coarse-scale conventional soil class map, we mapped our high-resolution soil class map using a Random Forest (RF) model. Modelling using RF is considered suitable for soil class mapping because of its robustness, and ability to produce reliable predictions, especially for non-linear relationships [53–56]. Nonetheless, we cannot exclude recent advancements and successes in soil class modelling, such as the use of artificial neural networks – ANNs [57–59].

We adopted the standard DSM approach, specifically the SCORPAN model, proposed by McBratney et al. [60] to fit an RF model, hence generating a high-resolution countrywide soil class map at 90 × 90 m/pixel (Fig. 3A). Based on the SCORPAN model, our covariates had to represent soil (S), climatic (C), organism/vegetation (O), relief (R), parent material (P), age/time factor (A), and space/geographical position (N). Also, we decided to select several covariates to better characterize soil diversity across Botswana, a massive landmass. Also, this ensured our RF model adapted effectively to landscape variations and remained flexible given varying contributions of covariates. The model employed the soil class observational point data ($n = 2060$) intersected with the covariates in Fig. 2B. We used the randomForest package in the software R to fit this RF model [61]. Our RF model was validated using a nested cross-validation approach, ensuring all the observational data was used. The nested cross-validation approach has proven reliable for reducing model bias and ensuring optimal hyperparameter tuning, especially in cases where the dataset is somewhat small [62]. The model accuracy results for our RF model showed an overall accuracy (OA) of 56.2 ± 3.3 % and a kappa statistic (KS) of 39.7 ± 4.6 % respectively. Our RF model's overall accuracy result mirrored other national scale results (*i.e.*, OA ranging from 40 to 70 %) previously published [58, 63–65]. We then used our RF model to map the soil classes across Botswana based on the covariate stack (Fig. 2B, Table 1) at the desired 90 m resolution.

With the countrywide 90 m resolution soil class map (Fig. 3A), we then estimated pedodiversity (Fig. 3B) as a continuum based on the RaO's quadratic entropy index method [66]. This method employs a moving window of N pixels, in our case 9 pixels for robustness, that traverses the countrywide soil class map to compute diversity estimates for all pixels [18]. Higher and lower diversity estimates represented higher and lower soil diversity, respectively. In addition to the moving window, this method explicitly considers the spatial distance between pixels while computing diversity, ensuring that the resulting map represents a continuous range of values [18]. We used the Euclidean distance metric because of its simplicity and interpretability [67]. We present the final RaO's quadratic entropy index equation here:

$$RaO\ QE = \sum_{i=1}^{n} \sum_{j=1}^{n} p_i p_j d_{ij}$$

Where:

n = The sum of soil classes across Botswana.

p_i and p_j = relative abundance of soil classes i and j across Botswana.

d_{ij} = The distance metric (*e.g.*, Euclidean, Cosine, *etc.*) used between soil classes i and j.

For further details and mathematical proofs regarding this equation, we refer to Rocchini et al. [66]. Since we wanted to examine the pedodiversity-elevation relationship, we also obtained an

Table 1
List of covariate layers used to map soil classes across Botswana.

Covariate Full Name	Abbreviation	Spatial Resolution	Unit of Measurement	Source
Above Ground Biomass	agb	100 m	Megagrams Per Hectare	https://catalogue.ceda.ac.uk/uuid/5f331c418e9f4935b8eb1b836f8a91b8
Aspect	aspect	90 m	Degrees	https://srtm.csi.cgiar.org/
Bare Soil Index	bsi	90 m	Unitless	[46]
Carbonate Index	cbi	90 m	Unitless	[47]
Clay Index	ci	90 m	Unitless	[47]
Clay Mineral Ratio	cmr	90 m	Unitless	http://pro.arcgis.com/en/pro-app/help/data/imagery/indices-gallery.htm
Distance from The Highest Elevation	dfhe	90 m	Meters	[48]
Distance from Lowest Elevation	dfle	90 m	Meters	[48]
Elevation	elevation	90 m	Meters	https://srtm.csi.cgiar.org/
Two-Band Enhanced Vegetation Index	evi2	90 m	Unitless	https://developers.google.com/earth-engine/datasets/catalog/LANDSAT_LC08_C02_T1_L2
Extractable Iron	extractable_fe	30 m	Parts Per Million	https://www.isda-africa.com/isdasoil/
Human Footprints	hfp_2013	1 km	Unitless	https://datadryad.org/stash/dataset/doi:10.5061/dryad.3tx95x6d9
Iron Oxide Ratio	ior	90 m	Unitless	http://pro.arcgis.com/en/pro-app/help/data/imagery/indices-gallery.htm
Aeromagnetics	magnetics	50 m	Nanoteslas	https://www.bgi.org.bw/
Modified Soil Adjusted Vegetation Index	msavi	90 m	Unitless	https://developers.google.com/earth-engine/datasets/catalog/LANDSAT_LC08_C02_T1_L2
Normalized Difference	ndvi	90 m	Unitless	https://developers.

(*continued on next page*)

Table 1 (*continued*)

Covariate Full Name	Abbreviation	Spatial Resolution	Unit of Measurement	Source
Vegetation Index				google.com/earth-engine/datasets/catalog/LANDSAT_LC08_C02_T1_L2
Normalized Difference Water Index	ndwi	90 m	Unitless	https://developers.google.com/earth-engine/datasets/catalog/LANDSAT_LC08_C02_T1_L2
Longitude	x-axis	90 m	Degrees	https://bitbucket.org/abmoeller/ogc/src/master/rPackage/OGC/
Latitude	y-axis	90 m	Degrees	https://bitbucket.org/abmoeller/ogc/src/master/rPackage/OGC/
Long-Term Mean Monthly Rainfall	rainfall	1 km	Millimeters	https://www.worldclim.org/data/index.html
Roughness	roughness	90 m	Degrees	https://srtm.csi.cgiar.org/
Soil Adjusted Vegetation Index	savi	90 m	Unitless	https://developers.google.com/earth-engine/datasets/catalog/LANDSAT_LC08_C02_T1_L2
Salinity Index	si	90 m	Unitless	[49,50]
Slope	slope	90 m	Degrees	https://srtm.csi.cgiar.org/
Long-Term Mean Monthly Temperature	temperature	1 km	Degrees Celsius	https://www.worldclim.org/data/index.html
Terrestrial Ecoregions	terr_ecosystems	~ 1: 111000*	Unitless	https://www.worldwildlife.org/publications/terrestrial-ecoregions-of-the-world

Footnote: All covariates except for the terrestrial ecoregions* map were resampled via the bilinear method to a common 90m resolution in the software R. The terrestrial ecoregions map was a multi-polygon vector layer which was first rasterized through the Rasterize function in QGIS Open Software and then resampled to 90m resolution via the nearest-neighbor method in the software R. Following the SCORPAN factors we group our covariates as follows: Soil (S): bsi, cbi, ci, cmr, extractable_fe, and si. Climate (C): rainfall and temperature. Organism/Vegetation (O): agb, evi2, hfp_2013, savi, msavi, ndvi, and ndwi. Relief (R): aspect, elevation, roughness, and slope. Parent Material (P): ior and magnetics. Age/Time Factor (A): terr_ecosystems. Space/Geographical Position (N): dfhe, dfle, x-axis and y-axis.

equal-resolution elevation map of Botswana from the Shuttle Radar Topography Mission (SRTM) (Figs. 2B and 3C). Using a bivariate mapping approach [68], we overlayed both countrywide 90 m resolution pedodiversity and elevation maps to visualize their spatial covariation (*i.e.*, high *versus* low-value assortment per variable) (Fig. 3D). Details on this approach are fully discussed in our previous study [69].

Having both countrywide 90 m resolution pedodiversity and elevation maps, we also created equivalent resolution maps for the two districts (Central and Southern) by masking each based on their shapefile. These two districts were chosen since they are the most populous regions in Botswana, and most landscape-related decisions are first benchmarked here before being implemented in other districts due to their widely diverse ecological contexts. We now had 90 m resolution maps for the entire country, including the Central and Southern districts. To account for differences in spatial resolutions, the 90 m resolution maps of pedodiversity and elevation across extents were aggregated to pixel sizes of 900, 9000, and 90,000 m, respectively. Such map aggregation involved taking the original 90 m resolution maps and multiplying them each time by powers of ten. For instance, $90 \times 10^{1} = 900$ m, $90 \times 10^{2} = 9000$ m, and $90 \times 10^{3} = 90{,}000$ m, respectively across the different spatial extents [30,31,70] . Next, using the geo-locations (*i.e.*, x and y coordinates) of the initial observational point data ($n = 2060$), we extracted the pedodiversity and elevation information per spatial extent as well as resolution. We should highlight here that as the spatial extent reduced, so did the number of observations due to the border shapefile effect. The countrywide extent included all $n = 2060$ observations, which were reduced to $n = 633$ for the Central district and $n = 100$ for the Southern district respectively.

The datasets we extracted were now used to relate pedodiversity and elevation across different spatial extents and resolutions. We used the Generalized Linear Model (GLM) and Geographically Weighted Regression Model (GWR) for this purpose. These models are inherently interpretable, allowing us to measure the strength (coefficient of determination) and direction (positive or negative) of the relationships between variables [71,72]. For the GLM, we fit a regression equation relating the two variables (pedodiversity ~ elevation, family = Gaussian) using the glm function from the MASS package in R [73]. We fit the GWR using the gwss function in the R package GWmodel [74,75]. The GWR enabled us to explore the spatial structures (*i.e.*, local mean estimates) and relationships (*i.e.*, local Pearson correlation estimates) of the two variables. For the GWR, we adopted the adaptive bandwidth, which is more flexible to the density of observations than a fixed bandwidth [76]. Here, we relied on domain or expert knowledge—also emphasized by [76]—to assign an appropriate bandwidth, keeping in mind that soil processes rely not just on nearby components but also on those farthest away. So, we first defined a fair number of neighbors, ranging from 30 to 50, based on the adequacy of our datasets and the need for robust estimates independent of distance or adaptive radius. Though computational to test different neighbors, the results maintained rather consistent spatial patterns, with slightly better outcomes near the 50-mark range. For this reason, we chose to settle for a bandwidth value somewhat less than 50. Once again, we refer to the workflow (Fig. 1) for clarity on the study's methodological procedures.

3. Results and discussion

Together, our findings show that the connection between pedogenesis factors, like elevation with pedodiversity is significantly affected by changes in spatial scale (*i.e.*, extent and resolution). The relationship becomes stronger as the area's spatial extent and resolution decrease, such as in the case of the Southern district. Our findings support the importance of considering spatial scale when analyzing the relationship between pedodiversity and elevation, as both factors are closely linked

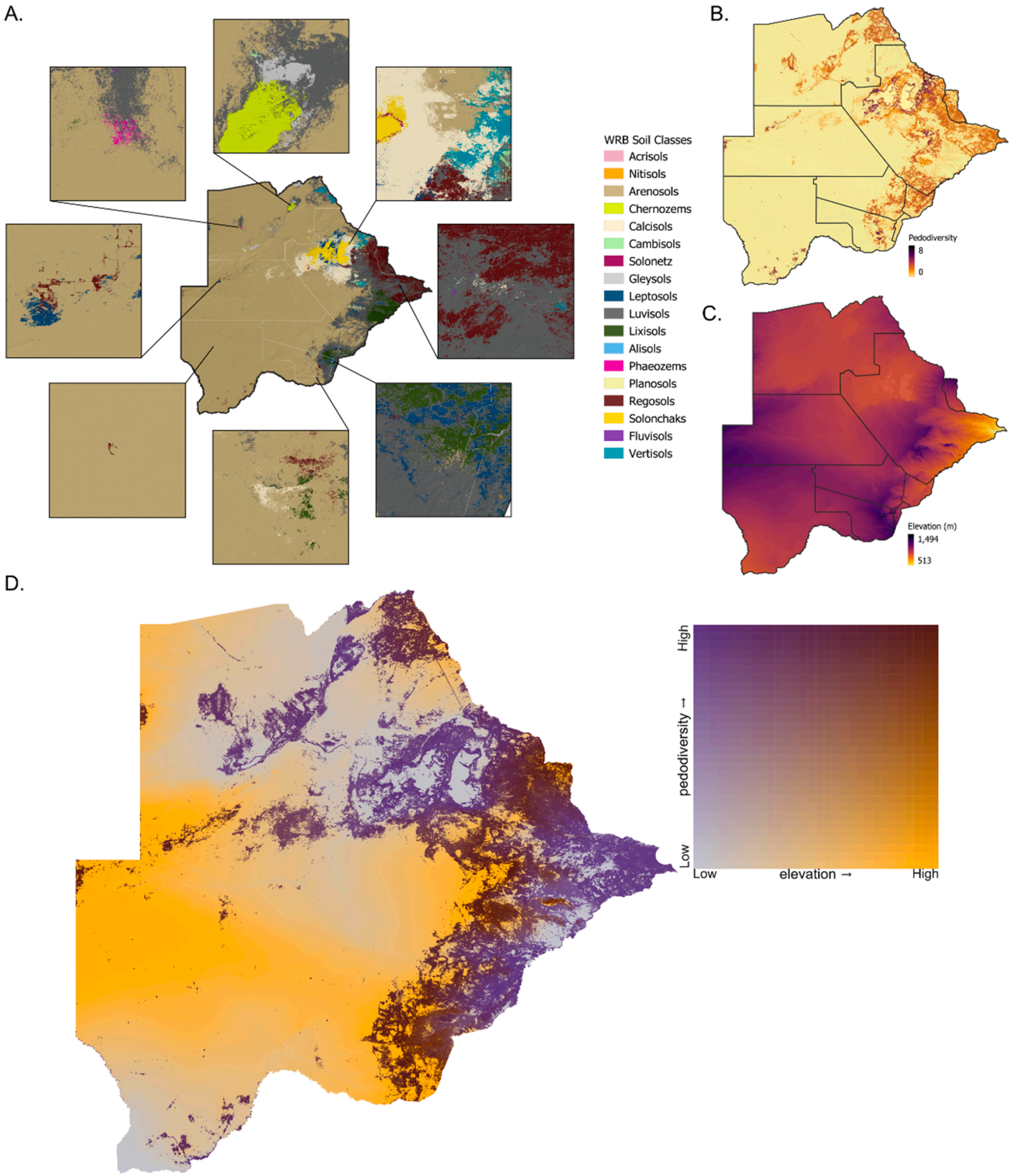

Fig. 3. Pedodiversity – elevation interplay in Botswana. (a) The random forest (RF) soil class map at 90 m × 90 m pixels with overall accuracy (OA) = 56.2 ± 3.3 % and kappa statistic (KS) = 39.7 ± 4.6 %, (b) RaO's quadratic entropy index documenting the alpha (α) diversity of the soil classes at 90 m × 90 m pixels, (c) The Shuttle Radar Topography Mission (SRTM) elevation layer at 90 m × 90 m pixels and (d) overlaps between the pedodiversity and elevation maps. [Note: Covariation between pedodiversity and elevation represent regions with low elevation-low pedodiversity (grey shade), low elevation-high pedodiversity (purple shade), high elevation-low pedodiversity (orange/yellow shade), and high elevation-high pedodiversity (brown/wine shade). All maps are based on the World Geodetic System (WGS) 1984 projection].

to various landscape features like vegetation. This underlines the need for stakeholders to develop landscape policies and frameworks that address multiple scales to effectively plan and make decisions.

3.1. Spatial covariation between pedodiversity and elevation

Elevation significantly influences the distribution of pedodiversity in Botswana. This was highlighted as one of the most important covariates in our RF model variable importance plot (refer to Fig. S1). Our analysis of the spatial covariation map revealed that the relationship between pedodiversity and elevation varies greatly across Botswana (Fig. 3D). Upon further investigation, we observed that the hardveld region in eastern Botswana exhibits higher pedodiversity (depicted by a purple shade) compared to the sandveld region in the west (depicted by an orange/yellow shade). This observation aligns with our expectation that the hardveld region's diverse soil classes contribute to its higher pedodiversity compared to the sandveld region [40]. Moreover, this also reflects distinct land cover types and optimal climatic conditions (Fig. 2B; Ringrose et al., 2002). Soils in the hardveld region are highly fertile allowing them to sustain more vegetation cover as well as human activities including cultivation and livestock rearing [42]. Meanwhile, the sandveld had low pedodiversity observed from the Arenosol deposit, which dominates most of the country. Most arid regions exhibit slower pedogenic activity [77] due to many factors (*e.g.*, erratic climatic conditions, and low vegetation cover), resulting in less diverse soils. However, this does not imply that arid soils do not undergo pedogenic processes, certain processes, like eluviation and salinization, may be in effect [78]. Meanwhile, elevation varied widely though showing mostly high values towards the western sandveld region.

In our observation of the two districts, we noticed that distinct soil classes corresponded with the spatial patterns of vegetation, climate, and elevation (refer to Figs. 2 and 3). The Central district contains most of the soil classes found in Botswana, such as Solonchaks, Solonets, Leptosols, Regosols, Lixisols, Luvisols, Vertisols, and Arenosols, resulting in higher pedodiversity. This district is more vegetated than the Southern district, and it has a higher proportion of lowlands compared to highlands (Fig. 3D). These lowlands are crucial for soil processes, such as soil carbon storage and sequestration, and they also help reduce the potential effects of erosion and land degradation. Meanwhile, the Southern district is characterized by soil classes like Acrisols and Nitisols that are not found in the Central district and it mostly undulates on highlands ranging between 1000 and 1300 m above sea level (Fig. 3D). High elevation may impact climatic conditions, influencing different soil processes such as organic matter decomposition or nutrient fluxes which strongly depend on temperature and rainfall variation or patterns [79–81]. The two districts receive different temperature and precipitation levels (Fig. 2B). While the Central district experiences high and low annual mean temperature variations depending on location, with typically moderate annual mean precipitation amounts between 400 and 700 mm per year, the Southern district has lower annual temperatures yet higher precipitation levels of about 800 mm. Precipitation affects different soil nutrient balances while also ensuring soils retain ample moisture to sustain plant growth [82,83]. Invariably, different factors are bound to affect pedodiversity and its response to elevational changes in these two districts.

3.2. Pedodiversity-elevation relationships inferred through statistical models

Our GWR results demonstrated that as the spatial resolution decreased, the local correlation between pedodiversity and elevation observational point data increased significantly. This phenomenon could not be attributed to the differences in spatial extent, as evidenced by Figs. 4, 5, and 6. Meanwhile, our GLMs for Botswana and the Central district unequivocally indicated a negative correlation between pedodiversity and elevation across various spatial resolutions (Figs. 4, 5, and 7). In contrast, for the Southern district, a clear positive correlation was observed (Figs. 6 and 7). Consistent with previous findings [9], our research in Botswana revealed a consistent decrease in pedodiversity as elevation increased. Across different spatial extents, this relationship became distinctly stronger as the spatial resolution decreased, displaying either positive or negative correlations, with R^2 values ranging from 0.00048 to 0.017 (National), 0.007 to 0.015 (Central), and 0.061 to 0.650 (Southern). Notably, the wide range of R^2 values indicates that the relationship between pedodiversity and elevation is weak for larger extents (Botswana) compared to smaller ones (Southern district). These results are linked to spatial averaging effects [84], leading to more simplified spatial distributions of pedodiversity and elevation throughout the country compared to within specific districts (see Fig. S2). Nevertheless, we acknowledge the imperative need for further research to seamlessly grasp the impact of spatial averaging effects on pedodiversity-elevation relationships. Such understanding will undoubtedly facilitate generalizing results across different scales and contribute to methodological advancements in comprehending and analyzing this significant relationship. We should also emphasize here that, a 90,000 m resolution is insufficient to capture the variability in the pedodiversity-elevation relationship specifically at the smallest extent (*i.e.*, southern district). However, by intentionally pushing the resolution to its limits, we also show the potential biases and limitations of using coarse resolutions for such small spatial extents when modelling pedodiversity or pedodiversity-elevation relationships. Here, our findings suggest that finer resolutions are necessary to accurately capture the variability at this extent. We also support our GWR and GLM model results through a non-parametric Spearman correlation approach which happens to capture fairly comparable relationships (Fig. 8).

Our findings show significant differences in landscape changes and variability across different spatial extents. We know that the distribution of pedodiversity does not only rely on elevation but also on a complex landscape system that involves various additional factors such as local human activities like agriculture. Elevation is a factor that affects soil on a local to medium scale. However, as mentioned earlier, other factors such as land cover types, which are primarily local, may also play a crucial role in driving pedodiversity, especially at the district level. These local-scale factors may have contrasting effects on pedodiversity. For example, there is evidence of pedodiversity reduction due to human-related alterations in a small town in Sicily, Italy [85]. It was found that soils once composed of different subgroups of Mollisol, Entisol, and Alfisol were now largely converted to a single anthropogenic soil class owing to prolonged cultivation. In contrast, some cultivation practices, including cover cropping and rotational cropping may favour overall soil quality [86] as well as limit soil erosion through runoff under steep slopes as shown by Durán Zuazo et al. [87]. These cropping systems when applied continuously have been shown to improve the chemical, biological, and physical properties of soil under different elevation gradients, all of which boost its capacity to function optimally [88,89]. By optimally, we mean the soil's ability to support key ecosystem services including controlling erosion facilitated by good structure or particle aggregation, nutrient cycling, and climate regulation [90]. All these are expected to affect pedodiversity locally, here particularly in the two districts.

Aside from land cover-related issues, localized landscape differences which comprise factors like aspect, slope variation, and microclimatic conditions [91] may result in variances in soils observed especially at the district levels. Such differences are important for vegetation (*e.g.*, annual grasses), which usually follow similar distributional patterns like microclimatic conditions, elevation, slope, and aspect [91,92]. Vegetation cover may reduce the chances of erosion by ensuring soil particles remain tightly held together hence limiting potential negative impacts on pedodiversity especially in hilly as well as semi-arid settings [93,94]. Meanwhile, microclimatic conditions may be associated with suitable conditions including enough sunlight, greater water availability, active soil microbial activity, and balanced nutrient amounts that enable the

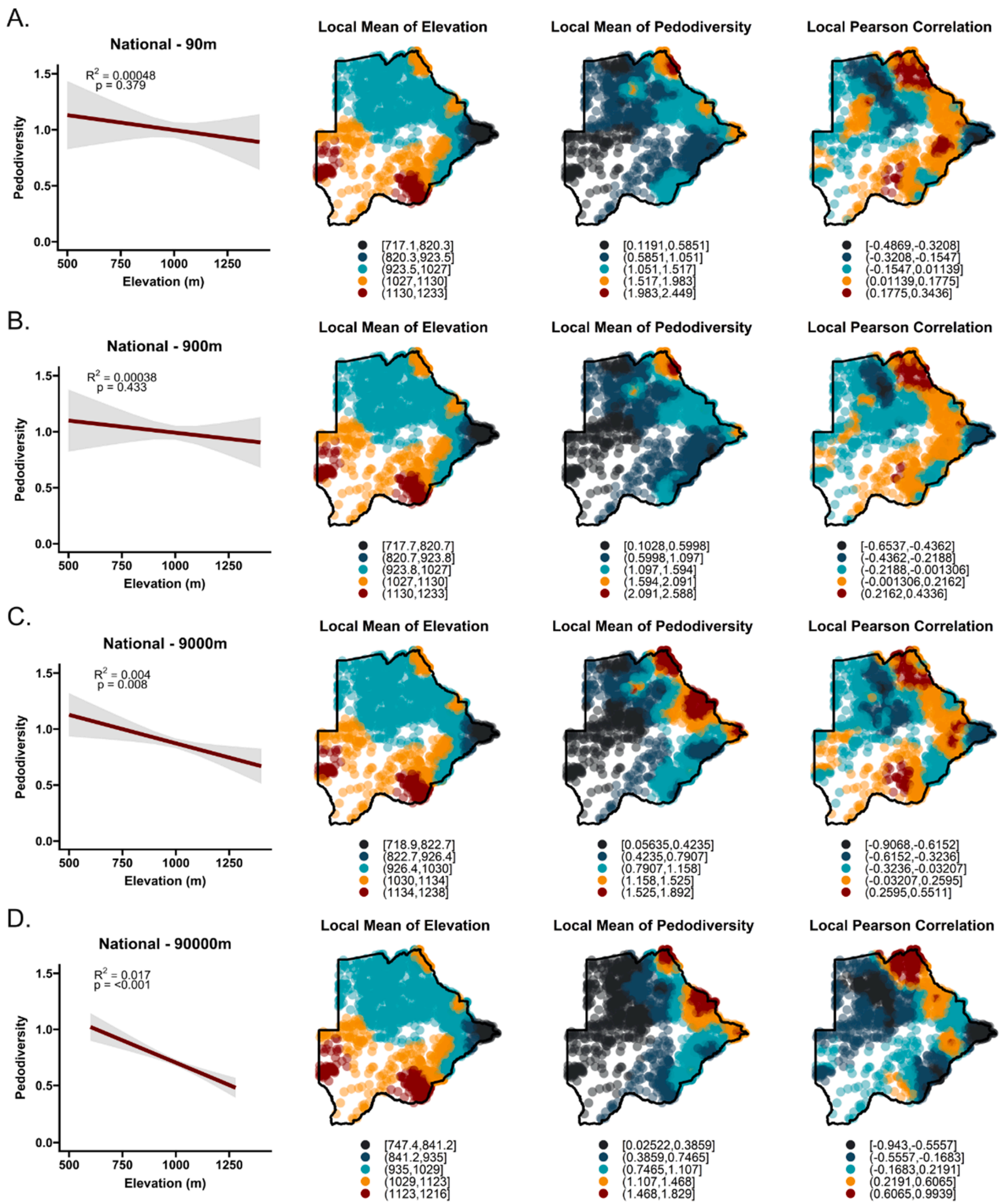

Fig. 4. National pedodiversity elevational relationships *via* generalized linear models (GLMs) across spatial resolution and corresponding geographically weighted (GWR) local summary statistical maps showing observational data point locations ($n = 2060$). [Note: Images A to D represent different spatial resolutions, 90 to 90,000 m respectively. The geographically weighted statistics from the maps are based on the default Gaussian kernel with a bandwidth of 48. Maps are based on the World Geodetic System (WGS) 1984 projection].

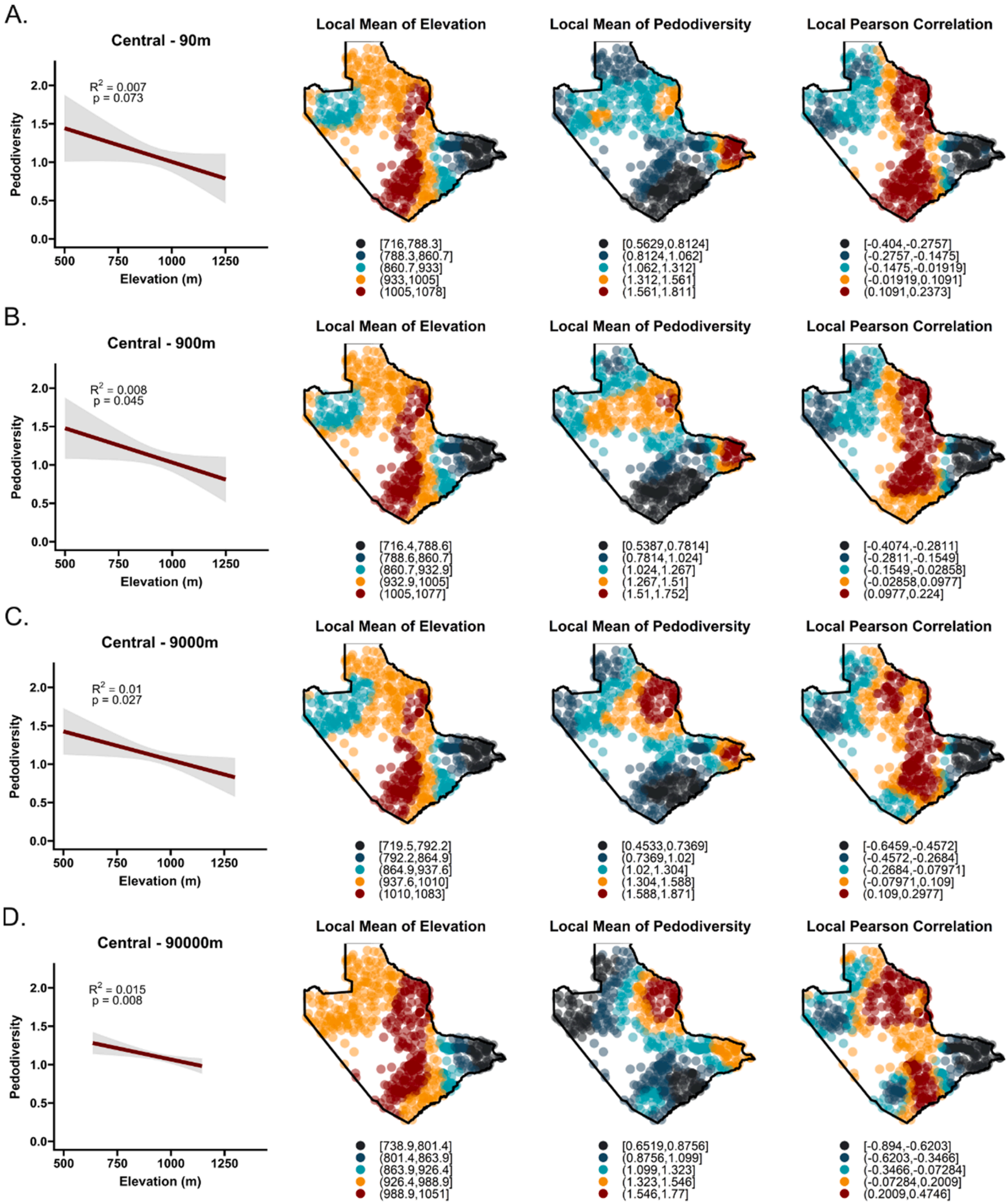

Fig. 5. Central district pedodiversity elevational relationships *via* generalized linear models (GLMs) across spatial resolutions and corresponding geographically weighted (GWR) local summary statistical maps showing observational data point locations ($n = 633$). [Note: Images A to D represent different spatial resolutions, 90 to 90,000 m respectively. The geographically weighted statistics from the maps are based on the default Gaussian kernel with a bandwidth of 48. Maps are based on the World Geodetic System (WGS) 1984 projection].

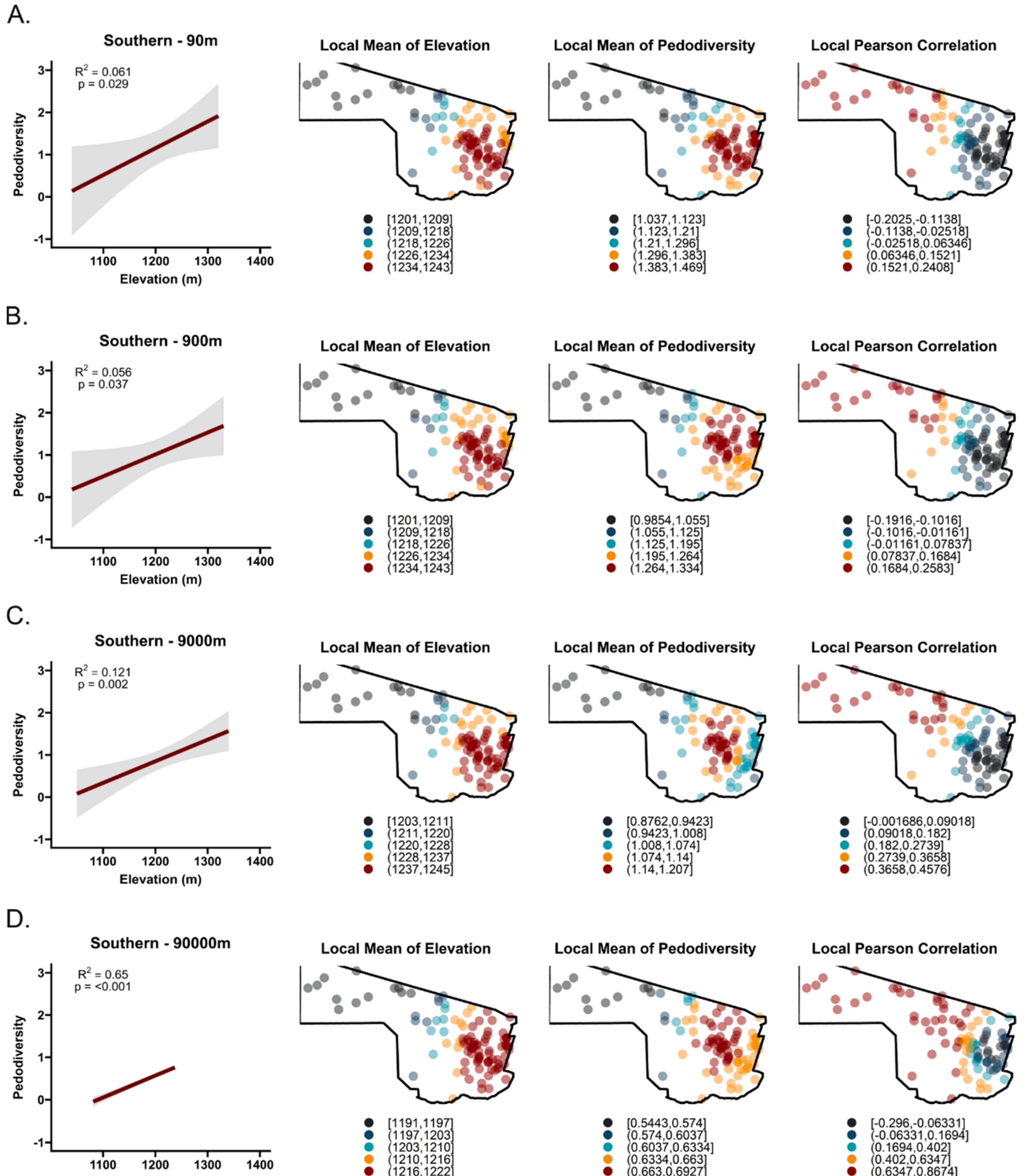

Fig. 6. Southern district pedodiversity elevational relationships *via* generalized linear models (GLMs) across spatial resolutions and corresponding geographically weighted (GWR) local summary statistical maps showing observational data point locations ($n = 100$). [Note: Images A to D represent different spatial resolutions, 90 to 90,000 m respectively. The geographically weighted statistics from the maps are based on the default Gaussian kernel with a bandwidth of 48. Maps are based on the World Geodetic System (WGS) 1984 projection].

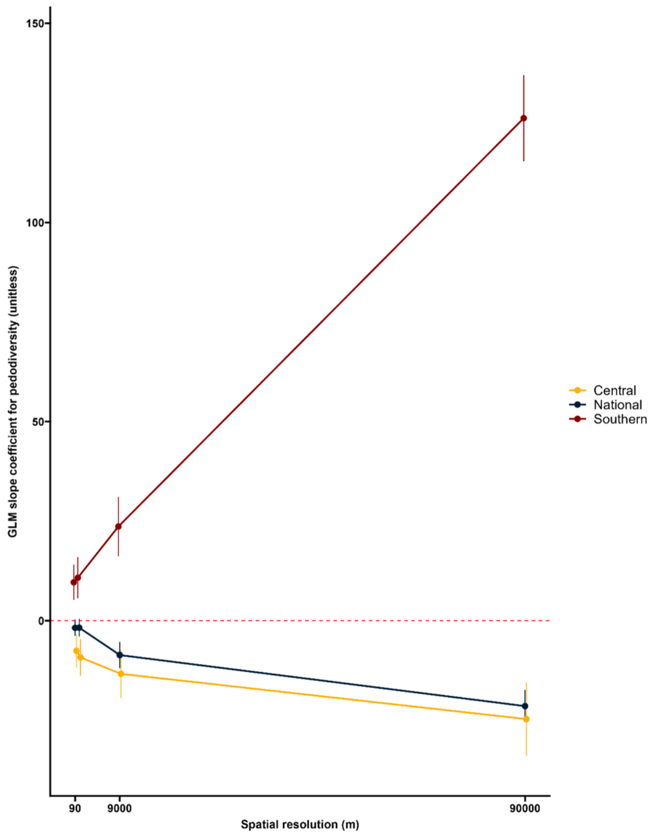

Fig. 7. Generalized linear models (GLMs) pedodiversity slope coefficients for respective scatter plots in Figs. 4, 5, and 6 *versus* spatial resolution in meters (m). [Note: The 900 m resolution could not be labelled on the x-axis to avoid overlaps since the graph tick is close to the 90 m tick. Error bars are the ± standard error estimates slightly offset to differentiate between the respective plots. Slope coefficients below the red dotted line are negative relative to the positive ones above].

support of biological groups ranging from mega- to micro-fauna and flora [95]. These suitable conditions may foster diverse, resilient, and highly fertile soils under varying elevations, hence contributing positively to pedodiversity. Microclimates are reliable in protecting forest biodiversity from climate change [96].

The Central district, being closer to the equator than the Southern district, supports greater plant cover (Fig. 2B) and consequently, more diverse soils due to higher solar energy reception [97]. Nonetheless, we also assume the same for the Southern district's most elevated areas (1250 to 1300 m; Fig. 2A), because certain plants growing at these altitudes may have access to enough solar energy. This may explain why some of the high-altitude areas of the Southern district have more diverse soils (Fig. 3B), apart from favourable climatic conditions (Fig. 2B). Plants use solar energy to produce their food through photosynthesis. This in turn supports plant growth. As plants develop, they contribute carbon both above- and below-ground through litterfall and rhizodeposition [98,99]. These processes promote the formation of nutrient-rich soils [100,101], and eventually diverse soils. Overall, even with varying spatial resolution, these different factors are expected to influence the pedodiversity-elevation relationship reported countrywide and across the two districts.

3.3. Semi-arid region characteristics in pedodiversity-elevation relationship

Semi-arid regions like Botswana are characterized by sparse vegetation patterns, recurrent soil erosion and deposition events, greatly varying soil moisture regimes, and erratic climate conditions. These affect the pedodiversity-elevation relationship in various ways. For instance, sparsely vegetated areas have lower plant cover which reduces soil protection. This exposes soils, leaving them more vulnerable to agents of erosion (*e.g.*, wind). In high-elevation areas, such exposure accelerates soil erosion, often leading to rapid deposition. Pedodiversity-elevation relationship is also affected by soil moisture regimes and ambient climatic conditions. As elevation increases, both ambient and soil temperatures become slightly cooler. Such cool temperatures affect microclimatic conditions and eventually soil composition. Together, these characteristics contribute to the diversity of soils in semi-arid regions.

3.4. Implications for operational purposes

Our results corroborate the following operational considerations: (1) the need to support the development and implementation of scale-specific interventions for conserving soils under elevational variations. Such interventions are critical in identifying areas where elevation might contribute to soil loss through processes like erosion. Scale-specific targeting of these areas may allow for the conservation of soils and other landscape features that are closely related to soils (*e.g.*, vegetation). Given our findings, particularly regarding the large spatial extents (*i.e.*, countrywide, and Central district), conservation efforts could focus on limiting soil degradation at higher elevations where pedodiversity is low. Meanwhile, for the small spatial extent where a positive relationship between pedodiversity and elevation is shown, conservation efforts might be directed toward safeguarding and enhancing diverse soils in higher-elevation regions. This brings up another key point (2) biodiversity conservation, which can be effectively achieved through landscape restoration programs aimed at safeguarding and enhancing the soil quality across different elevational scenarios. For the fine spatial resolution where a positive relationship between pedodiversity and elevation is shown (*i.e.*, Southern district), focused efforts to protect and conserve critical habitats could be put in place to ensure long-term benefit from natural resources (*i.e.*, soils, vegetation). Again, soil erosion is a pressing issue, thus, (3) emphasizing erosion control, which is critical for semi-arid regions due to their vulnerability to climatic extremes (*e.g.*, high maximum temperatures, aridity, drought) can help to ensure that different soils under varied elevational patterns are targeted to reduce any form of soil or sediment loss. Such losses may alter the soil's composition, thereby reducing pedodiversity. For all spatial extents, high pedodiversity regions require stringent measures limiting erosion and degradation of soils, while more generalized erosion strategies could be adopted for regions with lower pedodiversity.

4. Conclusion

Our study shows that the relationship between pedodiversity and elevation is highly dependent on the spatial scale, both the extent of an area and resolution. Specifically, we show that as both spatial resolution and extent decrease, the pedodiversity-elevation relationship strengthens. This relationship shifts from a negative to a positive correlation, capturing major environmental heterogeneity. These findings suggest that landscape management strategies in semi-arid regions should account for spatial scale to reliably monitor pedodiversity changes driven by elevation. This way, policy, and decision-makers can be able to account for variations in local scale factors, such as land use, microclimatic conditions, and slope. Overall, this study advances our understanding of scale-dependent pedodiversity-elevation relationships. Also, underscoring the importance of integrating scale for soil management and monitoring efforts in semi-arid settings.

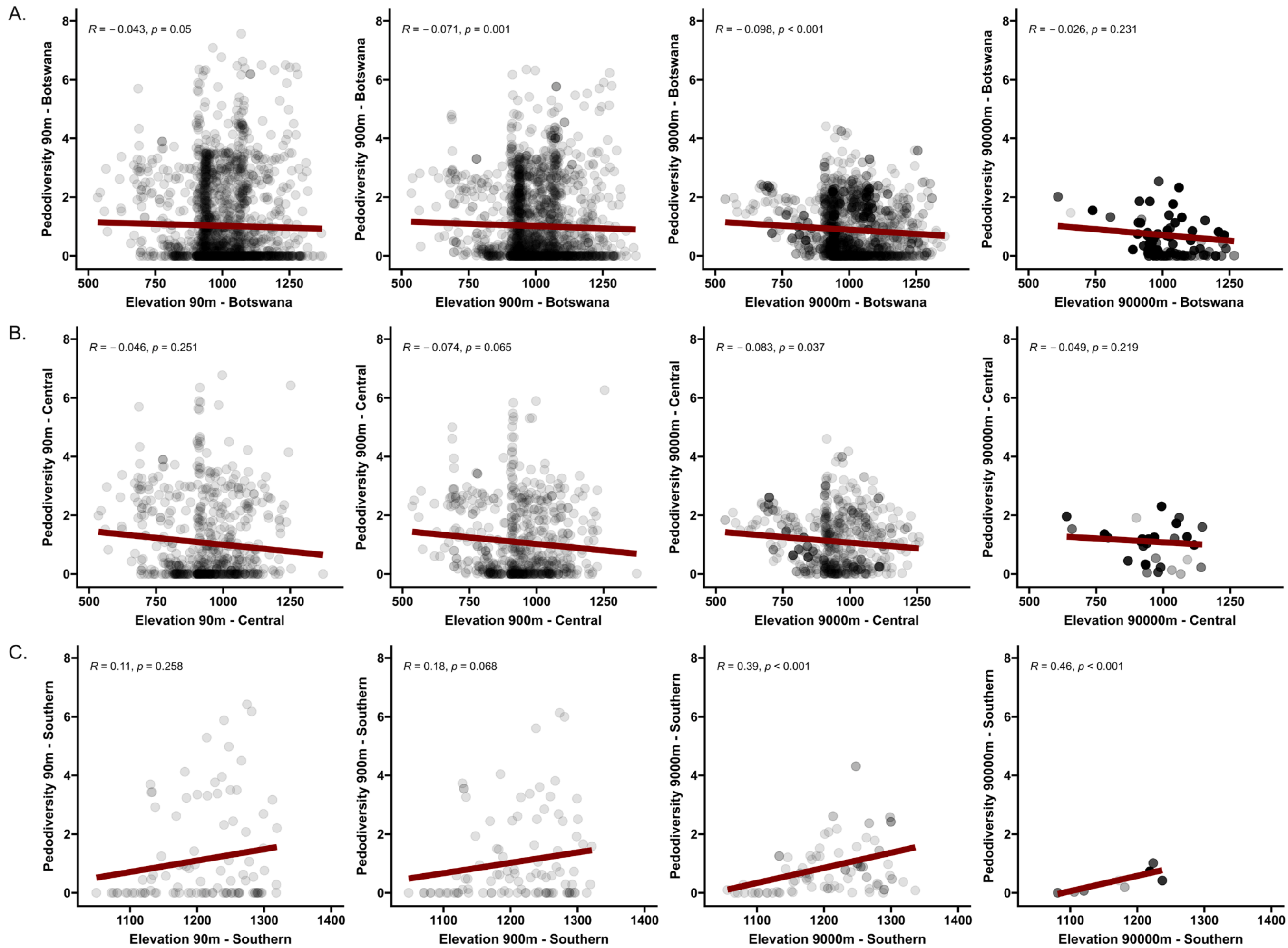

Fig. 8. Pedodiversity-elevation relationship across scales verified *via* non-parametric Spearman's correlation approach [Note: Results on the same row represent similar extent but vary sequentially based on resolution applied. The apparent reduction in points as you move from left to right occurs because they overlap due to the similarity in estimates of each variable – pedodiversity and elevation].

CRediT authorship contribution statement

Lesego Motlhetlhi: Writing – review & editing, Writing – original draft, Validation, Resources, Investigation, Data curation, Conceptualization. **Zibanani Seletlo:** Writing – review & editing, Writing – original draft, Software, Resources, Investigation, Data curation, Conceptualization. **Nafiseh Kakhani:** Writing – review & editing, Writing – original draft, Validation, Resources, Methodology, Data curation, Conceptualization. **Prince Chapman Agyeman:** Writing – review & editing, Writing – original draft, Validation, Resources, Methodology, Investigation, Data curation, Conceptualization. **John Kingsley:** Writing – review & editing, Writing – original draft, Software, Resources, Methodology, Investigation, Data curation, Conceptualization. **Ruhollah Taghizadeh-Mehrjardi:** Writing – review & editing, Writing – original draft, Visualization, Validation, Resources, Methodology, Investigation, Data curation, Conceptualization. **Ndiye Michael Kebonye:** Writing – review & editing, Writing – original draft, Visualization, Validation, Software, Resources, Project administration, Methodology, Investigation, Funding acquisition, Formal analysis, Data curation, Conceptualization. **Thomas Scholten:** Writing – review & editing, Writing – original draft, Visualization, Validation, Supervision, Resources, Project administration, Methodology, Investigation, Funding acquisition, Conceptualization. **Boineelo Moyo:** Writing – review & editing, Writing – original draft, Resources, Investigation, Conceptualization.

Declaration of Competing Interest

The authors in this work declare no competing interests.

Acknowledgement

The first author, N.M.K. was funded by the Deutsche Forschungsgemeinschaft (DFG, German Research Foundation) under Germany's Excellence Strategy – EXC number 2064/1 – Project number 390727645. This funding is greatly acknowledged. Also, we thank the Botswana Geoscience Institute (BGI) for the Aeromagnetic anomaly map.

Data and code availability

The codes used in this work together with the 90 m × 90 m soil class map of Botswana are available for download at: https://doi.org/10.5281/zenodo.14246108. We used most of the legacy soil class observational point data obtained from ISRIC Data Hub: https://data.isric.org/geonetwork/srv/eng/catalog.search#/metadata/b88870b4–6af8–4e78-a3ac-38871d757525. The remaining observational data were soil class centroids validated by Botswana's Ministry of Agriculture as part of the Botswana Range Inventory and Monitoring Project (BRIMP). The GWR codes were modified from: https://zia207.github.io/geospatial-r-github.io/geographically-weighted-summary-statistics.html. The map covariation code was adopted from: https://gist.github.com/scbrown86/2779137a9378df7b60afd23e0c45c188. The nested cross-validation code was modified from: https://dionysus.psych.wisc.edu/iaml_2020/unit-04.html#nested-cross-validation. The soil class mapping code was modified from: https://link.springer.com/book/10.1007/978–3-319–44327-0.

Appendix A. Supporting information

Supplementary data associated with this article can be found in the online version at doi:10.1016/j.geomat.2024.100037.

Data availability

The authors do not have the permission to share the data but have pointed readers where it can be requested from.

References

[1] D. Craven, M.T. van der Sande, C. Meyer, K. Gerstner, J.M. Bennett, D.P. Giling, J. Hines, H.R.P. Phillips, F. May, K.H. Bannar-Martin, J.M. Chase, P. Keil, A cross-scale assessment of productivity–diversity relationships, Glob. Ecol. Biogeogr. 29 (2020) 1940–1955, https://doi.org/10.1111/geb.13165.
[2] P.L. Zarnetske, Q.D. Read, S. Record, K.D. Gaddis, S. Pau, M.L. Hobi, S.L. Malone, J. Costanza, K. M. Dahlin, A.M. Latimer, A.M. Wilson, J.M. Grady, S.V. Ollinger, A.O. Finley, Towards connecting biodiversity and geodiversity across scales with satellite remote sensing, Glob. Ecol. Biogeogr. 28 (2019) 548–556, https://doi.org/10.1111/geb.12887.
[3] A. Chrobak, J. Novotný, P. Struś, Geodiversity Assessment as a First Step in Designating Areas of Geotourism Potential. Case Study: Western Carpathians, Front. Earth Sci. 9 (2021), https://doi.org/10.3389/feart.2021.752669.
[4] O. Scammacca, F. Bétard, G. Aertgeerts, A. Heuret, N. Fermet-Quinet, D. Montagne, Geodiversity assessment of french guiana: challenges and implications for sustainable land planning, Geoheritage 14 (2022) 83, https://doi.org/10.1007/s12371-022-00716-6.
[5] S. Pindral, R. Kot, P. Hulisz, The influence of city development on urban pedodiversity, Sci. Rep. 12 (2022) 6009, https://doi.org/10.1038/s41598-022-09903-5.
[6] J. Ibánez, S. Alba, Bermúdez, A. Garcia-Alvarez, Pedodiversity: Concepts and Measures, Catena 24 (1995), https://doi.org/10.1016/0341-8162(95)00028-Q.
[7] B. Minasny, A.B. McBratney, Incorporating taxonomic distance into spatial prediction and digital mapping of soil classes, Geoderma 142 (2007) 285–293, https://doi.org/10.1016/j.geoderma.2007.08.022.
[8] J.J. Ibáñez, J.G. Bockheim, Pedodiversity, CRC Press,, 2013.
[9] O. Vacek, R. Vašát, L. Borůvka, Quantifying the pedodiversity-elevation relations, Geoderma 373 (2020) 114441, https://doi.org/10.1016/j.geoderma.2020.114441.
[10] T. Fu, J. Liu, G. Jiang, H. Gao, F. Qi, F. Wang, Influences of pedodiversity on ecosystem services in a mountainous area, CATENA 217 (2022) 106505, https://doi.org/10.1016/j.catena.2022.106505.
[11] Y. Guo, P. Gong, R. Amundson, Pedodiversity in the United States of America, Geoderma 117 (2003) 99–115, https://doi.org/10.1016/S0016-7061(03)00137-X.
[12] T. Behrens, O. Schneider, G. Lösel, T. Scholten, V. Hennings, P. Felix-Henningsen, R. Hartwich, Analysis on pedodiversity and spatial subset representativity—the German soil map 1:1,000,000, J. Plant Nutr. Soil Sci. 172 (2009) 91–100, https://doi.org/10.1002/jpln.200700339.
[13] R. Vašát, O. Vacek, L. Borůvka, Studying the spatial structure of pedodiversity (Shannon's entropy) as related to the land area – An example from Czechia, Geoderma Reg. 32 (2023) e00607, https://doi.org/10.1016/j.geodrs.2023.e00607.
[14] J.J. Ibáñez, E. Feoli, Global Relationships of Pedodiversity and Biodiversity, Vadose Zone J. 12 (2013) vzj2012.0186, https://doi.org/10.2136/vzj2012.0186.
[15] H. Jenny, Factors of Soil Formation: A System of Quantitative Pedology, Dover,, New York, 1994.
[16] R. Scalenghe, S. Ferraris, The first forty years of a technosol, Pedosphere 19 (2009) 40–52, https://doi.org/10.1016/S1002-0160(08)60082-X.
[17] M. Luo, T. Wang, Z. Li, T. Zhang, J. Yang, N. Li, Z. Li, Spatial distribution characteristics of pedodiversity and its major driving factors in China based on analysis units of different sizes, CATENA 207 (2021) 105701, https://doi.org/10.1016/j.catena.2021.105701.
[18] D. Rocchini, M. Marcantonio, D. Da Re, G. Bacaro, E. Feoli, G.M. Foody, R. Furrer, R.J. Harrigan, D. Kleijn, M. Iannacito, J. Lenoir, M. Lin, M. Malavasi, E. Marchetto, R.S. Meyer, V. Moudry, F.D. Schneider, P. Šímová, A.H. Thornhill, E. Thouverai, S. Vicario, R.K. Wayne, C. Ricotta, From zero to infinity: Minimum to maximum diversity of the planet by spatio-parametric Rao's quadratic entropy, Glob. Ecol. Biogeogr. 30 (2021) 1153–1162, https://doi.org/10.1111/geb.13270.
[19] M. Berdugo, M. Delgado-Baquerizo, S. Soliveres, R. Hernández-Clemente, Y. Zhao, J.J. Gaitán, N. Gross, H. Saiz, V. Maire, A. Lehmann, M.C. Rillig, R. V. Solé, F.T. Maestre, Global ecosystem thresholds driven by aridity, Science 367 (2020) 787–790, https://doi.org/10.1126/science.aay5958.
[20] F.T. Maestre, M. Delgado-Baquerizo, T.C. Jeffries, D.J. Eldridge, V. Ochoa, B. Gozalo, J.L. Quero, M. García-Gómez, A. Gallardo, W. Ulrich, M.A. Bowker, T. Arredondo, C. Barraza-Zepeda, D. Bran, A. Florentino, J. Gaitán, J.R. Gutiérrez, E. Huber-Sannwald, M. Jankju, R.L. Mau, M. Miriti, K. Naseri, A. Ospina, I. Stavi, D. Wang, N.N. Woods, X. Yuan, E. Zaady, B.K. Singh, Increasing aridity reduces soil microbial diversity and abundance in global drylands, Proc. Natl. Acad. Sci. 112 (2015) 15684–15689, https://doi.org/10.1073/pnas.1516684112.
[21] M.K. Gaur, V.R. Squires, Geographic Extent and Characteristics of the World's Arid Zones and Their Peoples, in: M.K. Gaur, V.R. Squires (Eds.), Climate Variability Impacts on Land Use and Livelihoods in Drylands, Springer International Publishing, Cham, 2018, pp. 3–20, https://doi.org/10.1007/978-3-319-56681-8_1.
[22] P. Birkeland. Soils and Geomorphology, 3rd edition.,, Oxford University Press,, 1999. 〈https://global.oup.com/ushe/product/soils-and-geomorphology-9780195078862〉 (accessed June 16, 2024).
[23] M.C. Duniway, C. Benson, T.W. Nauman, A. Knight, J.B. Bradford, S.M. Munson, D. Witwicki, C. Livensperger, M. Van Scoyoc, T.T. Fisk, D. Thoma, M.E. Miller, Geologic, geomorphic, and edaphic underpinnings of dryland ecosystems: Colorado Plateau landscapes in a changing world, Ecosphere 13 (2022) e4273, https://doi.org/10.1002/ecs2.4273.
[24] T. Hengl, J.M. de Jesus, G.B.M. Heuvelink, M.R. Gonzalez, M. Kilibarda, A. Blagotić, W. Shangguan, M.N. Wright, X. Geng, B. Bauer-Marschallinger, M. A. Guevara, R. Vargas, R.A. MacMillan, N.H. Batjes, J.G.B. Leenaars, E. Ribeiro, I. Wheeler, S. Mantel, B. Kempen, SoilGrids250m: Global gridded soil information based on machine learning, PLOS ONE 12 (2017) e0169748, https://doi.org/10.1371/journal.pone.0169748.
[25] O. Scammacca, O. Sauzet, J. Michelin, P. Choquet, P. Garnier, B. Gabrielle, P. C. Baveye, D. Montagne, Effect of spatial scale of soil data on estimates of soil ecosystem services: Case study in 100 km2 area in France, Eur. J. Soil Sci. 74 (2023) e13359, https://doi.org/10.1111/ejss.13359.
[26] F. Liu, D.G. Rossiter, G.-L. Zhang, D.-C. Li, A soil colour map of China, Geoderma 379 (2020) 114556, https://doi.org/10.1016/j.geoderma.2020.114556.
[27] P. Krasilnikov, M. Gerasimova, D. Golovanov, M. Konyushkova, V. Sidorova, A. Sorokin, Pedodiversity and Its Significance in the Context of Modern Soil Geography, Eurasia Soil Sci. 51 (2018) 1–13, https://doi.org/10.1134/S1064229318010118.
[28] P.V. Krasilnikov, N.E. Garcia Calderon, A. Ibañez Huerta, Pedodiversity in mountainous tropical semideciduous forests of Sierra Madre del Sur, Mexico, Eurasia Soil Sc. 42 (2009) 1435–1442, https://doi.org/10.1134/S106422930913002X.
[29] G. Peterson, C.R. Allen, C.S. Holling, Ecological Resilience, Biodiversity, and Scale, Ecosystems 1 (1998) 6–18, https://doi.org/10.1007/s100219900002.
[30] T. Behrens, R.A. Viscarra Rossel, R. Kerry, R. MacMillan, K. Schmidt, J. Lee, T. Scholten, A.-X. Zhu, The relevant range of scales for multi-scale contextual spatial modelling, Sci. Rep. 9 (2019) 14800, https://doi.org/10.1038/s41598-019-51395-3.
[31] T. Behrens, K. Schmidt, R.A. MacMillan, R.A. Viscarra Rossel, Multi-scale digital soil mapping with deep learning, Sci. Rep. 8 (2018) 15244, https://doi.org/10.1038/s41598-018-33516-6.
[32] A. Bouasria, Y. Bouslihim, S. Gupta, R. Taghizadeh-Mehrjardi, T. Hengl, Predictive performance of machine learning model with varying sampling designs, sample sizes, and spatial extents, Ecol. Inform. 78 (2023) 102294, https://doi.org/10.1016/j.ecoinf.2023.102294.
[33] R.P. Bekker, P.V. de Wit, Vegetation Map of the Republic of Botswana. Soil mapping and Advisory Services project. AG:DP/BOT/85/011. - ESDAC - European Commission, (1990). https://esdac.jrc.ec.europa.eu/content/vegetation-map-republic-botswana-soil-mapping-and-advisory-services-project-agdpbot85011 (accessed June 16, 2024).
[34] T.M. Butynski, W. Von Richter, Wildlife Management in Botswana (1973-2006), Wildl. Soc. Bull. 3 (1975) 19–24.
[35] V. Kandjou, D.O. Nkwe, F. Ntuli, N. Keroletswe, Evaluating the degree of chemical contamination of underground aquifers in Botswana and analysing viable purification and desalination means; a review, Chem. Eng. Res. Des. 182 (2022) 216–224, https://doi.org/10.1016/j.cherd.2022.03.055.
[36] N. Batisani, F. Pule-Meulenberg, U. Batlang, F. Matteoli, N. Tselaesele, Retooling Smallholder Farming Systems for Climate Change Resilience Across Botswana Arid Zones, in: N. Oguge, D. Ayal, L. Adeleke, I. da Silva (Eds.), African Handbook of Climate Change Adaptation, Springer International Publishing, Cham, 2021, pp. 339–362, https://doi.org/10.1007/978-3-030-45106-6_168.
[37] N.M. Kebonye, Impact assessment of long term treated wastewater discharge on heavy metal concentration in soils from Palapye East, Botswana International University of Science and Technology (BIUST),, Botswana, Masters, 2017. 〈https://repository.biust.ac.bw/bitstream/handle/123456789/41/Kebonye_Ndiye%20Michael%202017.pdf?sequence=1〉. accessed June 17, 2024.
[38] B.L. Masocha, O. Dikinya, The Role of Poultry Litter and Its Biochar on Soil Fertility and Jatropha curcas L. Growth on Sandy-Loam Soil, Appl. Sci. 12 (2022) 12294, https://doi.org/10.3390/app122312294.
[39] E.N. Wilmsen, A. Griffiths, P. Thebe, D. Killick, G. Molatlhegi, Moijabana Rocks-Pilikwe Pots: The Acceleration of Clay Formation by Potters Employing Simple Mechanical Means, Ethnoarchaeology 8 (2016) 137–157, https://doi.org/10.1080/19442890.2016.1215885.
[40] P.N. Eze, Soil Development in the Eastern Hardveld, in: F.D. Eckardt (Ed.), Landscapes and Landforms of Botswana, Springer International Publishing, Cham, 2022, pp. 327–344, https://doi.org/10.1007/978-3-030-86102-5_19.

[41] N.M. Kebonye, P.N. Eze, P.C. Agyeman, K. John, S.K. Ahado, Efficiency of the t-distribution stochastic neighbor embedding technique for detailed visualization and modeling interactions between agricultural soil quality indicators, Biosyst. Eng. 210 (2021) 282–298, https://doi.org/10.1016/j.biosystemseng.2021.08.033.
[42] S. Ringrose, C. Vanderpost, W. Matheson, Seasonal Declines in Rangeland Quality in the Cultivated Hardveld of Botswana Using Landsat Thematic Mapper Imagery, Geocarto Int. 17 (2002), https://doi.org/10.1080/10106040208542233.
[43] G. Letlole, B. Gabalape, Botswana Geographical Names, (2016). ⟨https://unstats.un.org/unsd/geoinfo/ungegn/docs/29th-gegn-docs/exhibition/Botswana%20Geographical%20Names_REVISED.pdf⟩ (accessed March 20, 2023).
[44] J.G.B. Leenaars, B. Kempen, A. van Oostrum, N. Batjes, Africa Soil Profiles Database: a compilation of georeferenced and standardised legacy soil profile data for Sub-Saharan Africa, in: GlobalSoilMap: Basis of the Global Spatial Soil Information System - Proceedings of the 1st GlobalSoilMap Conference, 2014: pp. 51–57. https://doi.org/10.1201/b16500–13.
[45] J.I. Molefe, Characterization of Fire Regime Descriptors in Botswana Using Remotely Sensed Data, Handbook of Research on Geospatial Science and Technologies (2018) 86–100. https://doi.org/10.4018/978–1-5225–3440-2.ch005.
[46] C.T. Nguyen, A. Chidthaisong, P. Kieu Diem, L.-Z. Huo, A Modified Bare Soil Index to Identify Bare Land Features during Agricultural Fallow-Period in Southeast Asia Using Landsat 8, Land 10 (2021) 231, https://doi.org/10.3390/land10030231.
[47] R. Taghizadeh-Mehrjardi, B. Minasny, F. Sarmadian, B.P. Malone, Digital mapping of soil salinity in Ardakan region, central Iran, Geoderma 213 (2014) 15–28, https://doi.org/10.1016/j.geoderma.2013.07.020.
[48] T. Behrens, K. Schmidt, R.A. Viscarra Rossel, P. Gries, T. Scholten, R. A. MacMillan, Spatial modelling with Euclidean distance fields and machine learning, Eur. J. Soil Sci. 69 (2018) 757–770, https://doi.org/10.1111/ejss.12687.
[49] E. Asfaw, K.V. Suryabhagavan, M. Argaw, Soil salinity modeling and mapping using remote sensing and GIS: The case of Wonji sugar cane irrigation farm, Ethiopia, J. Saudi Soc. Agric. Sci. 17 (2018) 250–258, https://doi.org/10.1016/j.jssas.2016.05.003.
[50] M.M.E.-S. Gad, M.H.A. Mohamed, M.R. Mohamed, Soil salinity mapping using remote sensing and GIS, Geomatica 75 (2021) 295–309, https://doi.org/10.1139/geomat-2021-0015.
[51] P.De Wit, F. Nachtergaele, Soil Map of the Republic of Botswana. Soil Mapping and Advisory Services Project FAO/BOT/85/011. Map 1 of 2. - ESDAC - European Commission, (1990). ⟨https://esdac.jrc.ec.europa.eu/content/soil-map-republic-botswana-soil-mapping-and-advisory-services-project-faobot85011-map-1–2⟩ (accessed June 17, 2024).
[52] S. Grunwald, J.A. Thompson, J.L. Boettinger, Digital Soil Mapping and Modeling at Continental Scales: Finding Solutions for Global Issues, Soil Sci. Soc. Am. J. 75 (2011) 1201–1213, https://doi.org/10.2136/sssaj2011.0025.
[53] E.C. Brevik, C. Calzolari, B.A. Miller, P. Pereira, C. Kabala, A. Baumgarten, A. Jordán, Soil mapping, classification, and pedologic modeling: History and future directions, Geoderma 264 (2016) 256–274, https://doi.org/10.1016/j.geoderma.2015.05.017.
[54] C.W. Brungard, J.L. Boettinger, M.C. Duniway, S.A. Wills, T.C. Edwards, Machine learning for predicting soil classes in three semi-arid landscapes, Geoderma 239–240 (2015) 68–83, https://doi.org/10.1016/j.geoderma.2014.09.019.
[55] R. Grimm, T. Behrens, M. Märker, H. Elsenbeer, Soil organic carbon concentrations and stocks on Barro Colorado Island — Digital soil mapping using Random Forests analysis, Geoderma 146 (2008) 102–113, https://doi.org/10.1016/j.geoderma.2008.05.008.
[56] B. Heung, H.C. Ho, J. Zhang, A. Knudby, C.E. Bulmer, M.G. Schmidt, An overview and comparison of machine-learning techniques for classification purposes in digital soil mapping, Geoderma 265 (2016) 62–77, https://doi.org/10.1016/j.geoderma.2015.11.014.
[57] T. Behrens, H. Förster, T. Scholten, U. Steinrücken, E.-D. Spies, M. Goldschmitt, Digital soil mapping using artificial neural networks, J. Plant Nutr. Soil Sci. 168 (2005) 21–33, https://doi.org/10.1002/jpln.200421414.
[58] M. Fantappiè, G. L'Abate, C. Schillaci, E.A.C. Costantini, Digital soil mapping of Italy to map derived soil profiles with neural networks, Geoderma Reg. 32 (2023) e00619, https://doi.org/10.1016/j.geodrs.2023.e00619.
[59] K. Rau, K. Eggensperger, F. Schneider, P. Hennig, T. Scholten, How can we quantify, explain, and apply the uncertainty of complex soil maps predicted with neural networks? Sci. Total Environ. 944 (2024) 173720 https://doi.org/10.1016/j.scitotenv.2024.173720.
[60] A.B. McBratney, M.L. Mendonça Santos, B. Minasny, On digital soil mapping, Geoderma 117 (2003) 3–52, https://doi.org/10.1016/S0016-7061(03)00223-4.
[61] L. Breiman, A. Cutler, randomForest: Breiman and Cutler's Random Forests for Classification and Regression, (2018). ⟨https://CRAN.R-project.org/package=randomForest⟩ (accessed April 18, 2021).
[62] S. Varma, R. Simon, Bias in error estimation when using cross-validation for model selection, BMC Bioinforma. 7 (2006) 91, https://doi.org/10.1186/1471-2105-7-91.
[63] K. Adhikari, B. Minasny, M.B. Greve, M.H. Greve, Constructing a soil class map of Denmark based on the FAO legend using digital techniques, Geoderma 214–215 (2014) 101–113, https://doi.org/10.1016/j.geoderma.2013.09.023.
[64] L. Pásztor, A. Laborczi, Z. Bakacsi, J. Szabó, G. Illés, Compilation of a national soil-type map for Hungary by sequential classification methods, Geoderma 311 (2018) 93–108, https://doi.org/10.1016/j.geoderma.2017.04.018.
[65] R. Taghizadeh-Mehrjardi, K. Schmidt, K. Eftekhari, T. Behrens, M. Jamshidi, N. Davatgar, N. Toomanian, T. Scholten, Synthetic resampling strategies and machine learning for digital soil mapping in Iran, Eur. J. Soil Sci. 71 (2020) 352–368, https://doi.org/10.1111/ejss.12893.
[66] D. Rocchini, M. Marcantonio, C. Ricotta, Measuring Rao's Q diversity index from remote sensing: An open source solution, Ecol. Indic. 72 (2017) 234–238, https://doi.org/10.1016/j.ecolind.2016.07.039.
[67] P.-E. Danielsson, Euclidean distance mapping, Comput. Graph. Image Process. 14 (1980) 227–248, https://doi.org/10.1016/0146-664X(80)90054-4.
[68] B.E. Trumbo, A theory for coloring bivariate statistical maps, Am. Stat. 35 (1981) 220–226, https://doi.org/10.2307/2683294.
[69] N.M. Kebonye, P.C. Agyeman, Z. Seletlo, P.N. Eze, On exploring bivariate and trivariate maps as visualization tools for spatial associations in digital soil mapping: A focus on soil properties, Precis. Agric. 24 (2023) 511–532, https://doi.org/10.1007/s11119-022-09955-7.
[70] B. Kempen, D.J. Brus, G.B.M. Heuvelink, J.J. Stoorvogel, Updating the 1:50,000 Dutch soil map using legacy soil data: A multinomial logistic regression approach, Geoderma 151 (2009) 311–326, https://doi.org/10.1016/j.geoderma.2009.04.023.
[71] A.J. Dobson, A.G. Barnett. An Introduction to Generalized Linear Models, 4th ed..,, Chapman and Hall/CRC,, New York, 2018, https://doi.org/10.1201/9781315182780.
[72] P.A. Rogerson, A.S. Fotheringham, The SAGE Handbook of Spatial Analysis, SAGE,, 2008. ⟨https://www.torrossa.com/en/resources/an/4913744⟩ (accessed June 18, 2024).
[73] B. Ripley, B. Venables, D.M. Bates, K.H. (partial port ca 1998), A.G. (partial port ca 1998), D.F. (support functions for polr), MASS: Support Functions and Datasets for Venables and Ripley's MASS, (2024). https://cran.r-project.org/web/packages/MASS/index.html (accessed June 18, 2024).
[74] B. Lu, P. Harris, M. Charlton, C. Brunsdon, T. Nakaya, D. Murakami, I. Gollini, Y. Hu, F.H. Evans, GWmodel: Geographically-Weighted Models, (2024). https://cran.r-project.org/web/packages/GWmodel/index.html (accessed June 18, 2024).
[75] B. Lu, P. Harris, M. Charlton, C. Brunsdon, The GWmodel R package: further topics for exploring spatial heterogeneity using geographically weighted models, Geo-Spat. Inf. Sci. 17 (2014) 85–101, https://doi.org/10.1080/10095020.2014.917453.
[76] A. Comber, C. Brunsdon, M. Charlton, G. Dong, R. Harris, B. Lu, Y. Lü, D. Murakami, T. Nakaya, Y. Wang, P. Harris, A Route Map for Successful Applications of Geographically Weighted Regression, Geogr. Anal. 55 (2023) 155–178, https://doi.org/10.1111/gean.12316.
[77] A.L. Alexandrovskiy, Rates of soil-forming processes in three main models of pedogenesis, Rev. Mex. De. Cienc. Geológicas 24 (2007) 283–292.
[78] J. Walk, P. Schulte, M. Bartz, A. Binnie, M. Kehl, R. Mörchen, X. Sun, G. Stauch, C. Tittmann, R. Bol, H. Brückner, F. Lehmkuhl, Pedogenesis at the coastal arid-hyperarid transition deduced from a Late Quaternary chronosequence at Paposo, Atacama Desert, CATENA 228 (2023) 107171, https://doi.org/10.1016/j.catena.2023.107171.
[79] M.U.F. Kirschbaum, The temperature dependence of soil organic matter decomposition, and the effect of global warming on soil organic C storage, Soil Biol. Biochem. 27 (1995) 753–760, https://doi.org/10.1016/0038-0717(94)00242-S.
[80] N.C. Pepin, E. Arnone, A. Gobiet, K. Haslinger, S. Kotlarski, C. Notarnicola, E. Palazzi, P. Seibert, S. Serafin, W. Schöner, S. Terzago, J.M. Thornton, M. Vuille, C. Adler, Climate changes and their elevational patterns in the mountains of the world, e2020RG000730, Rev. Geophys. 60 (2022), https://doi.org/10.1029/2020RG000730.
[81] Z. Yuan, F. Jiao, X. Shi, J. Sardans, F.T. Maestre, M. Delgado-Baquerizo, P. B. Reich, J. Peñuelas, Experimental and observational studies find contrasting responses of soil nutrients to climate change, eLife 6 (2017) e23255, https://doi.org/10.7554/eLife.23255.
[82] R. Sehler, J. Li, J. Reager, H. Ye, Investigating relationship between soil moisture and precipitation globally using remote sensing observations, J. Contemp. Water Res. Educ. 168 (2019) 106–118, https://doi.org/10.1111/j.1936-704X.2019.03324.x.
[83] X.-Y. Zhang, Q.-W. Li, J.-Q. Gao, Y.-H. Hu, M.-H. Song, Y. Yue, Effects of rainfall amount and frequency on soil nitrogen mineralization in Zoigê alpine wetland, Eur. J. Soil Biol. 97 (2020) 103170, https://doi.org/10.1016/j.ejsobi.2020.103170.
[84] D.E. Jelinski, J. Wu, The modifiable areal unit problem and implications for landscape ecology, Landsc. Ecol. 11 (1996) 129–140, https://doi.org/10.1007/BF02447512.
[85] G. Lo Papa, V. Palermo, C. Dazzi, Is land-use change a cause of loss of pedodiversity? The case of the Mazzarrone study area, Sicily, Geomorphology 135 (2011) 332–342, https://doi.org/10.1016/j.geomorph.2011.02.015.
[86] C.S. Weerasekara, R.P. Udawatta, C.J. Gantzer, R.J. Kremer, S. Jose, K.S. Veum, Effects of Cover Crops on Soil Quality: Selected Chemical and Biological Parameters, Commun. Soil Sci. Plant Anal. 48 (2017) 2074–2082, https://doi.org/10.1080/00103624.2017.1406103.
[87] V.H. Durán Zuazo, J.R.F. Martínez, C.R.R. Pleguezuelo, A. Martínez Raya, B. C. Rodríguez, Soil-erosion and runoff prevention by plant covers in a mountainous area (se spain): Implications for sustainable agriculture, Environmentalist 26 (2006) 309–319, https://doi.org/10.1007/s10669-006-0160-4.

[88] S.M. Dabney, J.A. Delgado, D.W. Reeves, USING WINTER COVER CROPS TO IMPROVE SOIL AND WATER QUALITY, Commun. Soil Sci. Plant Anal. (2001), https://doi.org/10.1081/CSS-100104110.
[89] B. Volsi, G.E. Higashi, I. Bordin, T.S. Telles, The diversification of species in crop rotation increases the profitability of grain production systems, Sci. Rep. 12 (2022) 19849, https://doi.org/10.1038/s41598-022-23718-4.
[90] A. Ledo, P. Smith, A. Zerihun, J. Whitaker, J.L. Vicente-Vicente, Z. Qin, N. P. McNamara, Y.L. Zinn, M. Llorente, M. Liebig, M. Kuhnert, M. Dondini, A. Don, E. Diaz-Pines, A. Datta, H. Bakka, E. Aguilera, J. Hillier, Changes in soil organic carbon under perennial crops, Glob. Change Biol. 26 (2020) 4158–4168, https://doi.org/10.1111/gcb.15120.
[91] S.P. Hardegree, A.R. Boehm, N.F. Glenn, R.L. Sheley, P.A. Reeves, N.J. Pastick, A. Hojjati, S.P. Boyte, J. Enterkine, C.A. Moffet, G.N. Flerchinger, Elevation and Aspect Effects on Soil Microclimate and the Germination Timing of Fall-Planted Seeds, Rangel. Ecol. Manag. 85 (2022) 15–27, https://doi.org/10.1016/j.rama.2022.08.003.
[92] N.B. Schwartz, D. Medvigy, J. Tijerin, D. Pérez-Aviles, D. Rivera-Polanco, D. Pereira, G. Vargas G, L. Werden, D. Du, L. Arnold, J.S. Powers, Intra-annual variation in microclimatic conditions in relation to vegetation type and structure in two tropical dry forests undergoing secondary succession, For. Ecol. Manag. 511 (2022) 120132, https://doi.org/10.1016/j.foreco.2022.120132.
[93] M. Ruiz-Colmenero, R. Bienes, D.J. Eldridge, M.J. Marques, Vegetation cover reduces erosion and enhances soil organic carbon in a vineyard in the central Spain, CATENA 104 (2013) 153–160, https://doi.org/10.1016/j.catena.2012.11.007.
[94] G.-L. Wu, Y.-F. Liu, Z. Cui, Y. Liu, Z.-H. Shi, R. Yin, P. Kardol, Trade-off between vegetation type, soil erosion control and surface water in global semi-arid regions: A meta-analysis, J. Appl. Ecol. 57 (2020) 875–885, https://doi.org/10.1111/1365-2664.13597.
[95] R.H. Waring, S.W. Running, Forest Ecosystems: Analysis at Multiple Scales, Elsevier,, 2010.
[96] P. Sanczuk, K. De Pauw, E. De Lombaerde, M. Luoto, C. Meeussen, S. Govaert, T. Vanneste, L. Depauw, J. Brunet, S.A.O. Cousins, C. Gasperini, P.-O. Hedwall, G. Iacopetti, J. Lenoir, J. Plue, F. Selvi, F. Spicher, J. Uria-Diez, K. Verheyen, P. Vangansbeke, P. De Frenne, Microclimate and forest density drive plant population dynamics under climate change, Nat. Clim. Chang. 13 (2023) 840–847, https://doi.org/10.1038/s41558-023-01744-y.
[97] H. Poorter, Ü. Niinemets, N. Ntagkas, A. Siebenkäs, M. Mäenpää, S. Matsubara, ThijsL. Pons, A meta-analysis of plant responses to light intensity for 70 traits ranging from molecules to whole plant performance, N. Phytol. 223 (2019) 1073–1105, https://doi.org/10.1111/nph.15754.
[98] M. Neumann, L. Ukonmaanaho, J. Johnson, S. Benham, L. Vesterdal, R. Novotný, A. Verstraeten, L. Lundin, A. Thimonier, P. Michopoulos, H. Hasenauer, Quantifying Carbon and Nutrient Input From Litterfall in European Forests Using Field Observations and Modeling, Glob. Biogeochem. Cycles 32 (2018) 784–798, https://doi.org/10.1029/2017GB005825.
[99] S.H. Villarino, P. Pinto, R.B. Jackson, G. Piñeiro, Plant rhizodeposition: A key factor for soil organic matter formation in stable fractions, eabd3176, Sci. Adv. 7 (2021), https://doi.org/10.1126/sciadv.abd3176.
[100] D. Kerdraon, J. Drewer, A.Y.C. Chung, N. Majalap, E.M. Slade, L. Bréchet, A. Wallwork, B. Castro-Trujillo, E.J. Sayer, Litter inputs, but not litter diversity, maintain soil processes in degraded tropical forests—a cross-continental comparison, Front. . Glob. Change 2 (2020), https://doi.org/10.3389/ffgc.2019.00090.
[101] X. Wei, Y. Yang, Y. Shen, Z. Chen, Y. Dong, F. Wu, L. Zhang, Effects of litterfall on the accumulation of extracted soil humic substances in subalpine forests, Front. Plant Sci. 11 (2020), https://doi.org/10.3389/fpls.2020.00254.